DEVELOPMENT OF A HUMAN FE MODEL FOR ELDERLY FEMALE OCCUPANTS IN SIDE CRASHES

Hisaki Sugaya, Yukou Takahashi, Yasuaki Gunji, Yasuhiro Dokko
Honda R&D Co., Ltd. Automobile R&D Center
Japan

Murthy Ayyagari, Bryant Whitcomb, Craig Markusic
Honda R&D Americas, Inc.
United States

Amanda Agnew, Yun-Seok Kang, John Bolte IV
Injury Biomechanics Research Center (IBRC), The Ohio State University
United States

Paper Number 19-0052

ABSTRACT

A high fatality rate of the elderly in traffic crashes is an important issue to consider when facing an aging society in the future. Left side impacts have been found to be the most frequent when considering severe crashes involving elderly people that resulted in Abbreviated Injury Scale (AIS) 4+ injuries in the United States. Additionally, the frequency of rib fractures in female occupants is significantly higher than males in those over sixty years in a side impact. Therefore, there is a need to reduce rib fractures in elderly females in side impacts, which should significantly decrease the number of fatalities in these types of crashes. Currently there are no evaluation tools for elderly female occupants with increased fragility. The objective of this study was to develop a Human Body Model (HBM) of an elderly female with increased fragility to use in simulations which focus on side impacts.

The material properties of rib cortical bone were determined using average data from published literatures. A rib bending simulation was conducted to compare force-deflection response with published experimental data. The rib cortex model included thirty-two sections of a rib, in which the thickness of each section was determined by comparing to published precise cross-sectional data. The evaluated rib model was then applied to the full-body HBM of an elderly male which was developed in a past study. Using the full body model geometrically scaled to elderly female, published side impact sled tests at 28 km/h of delta-V with post mortem human subjects were simulated to compare kinematics, rib fracture locations, and thoracic deflection obtained from chest band data. Comparison of the force-deflection response of the rib in bending showed that the simulation result fell within the overall experimental range. In the side impact sled simulations, the predicted trajectories of T1, T12, and the pelvis were found to be similar to those from the experiment. The number of rib fractures, fracture timing, fracture locations and overall thoracic deflection in the simulation exhibited a similar trend to the experimental data.

The HBM developed by applying rib material properties and geometrical scaling for an elderly female well represented upper body kinematics, rib fractures and thoracic deflection in a side impact when compared to published PMHS experiments.

INTRODUCTION

The National Highway Traffic Safety Administration (NHTSA) reported the elderly population, age 65 or older, in the U.S. reached 47.8 million in 2015; this is nearly 15 percent of the total U.S. population [1]. Also, the number of licensed elderly drivers increased by 33% from 2006 to 2015, reaching 40.1 million. Furthermore, Ortman et al. [2] predicted that the elderly population will expand to 83.7 million by the year 2050. NHTSA also reported the number of elderly fatalities increased by 3% from 2006 to 2015, even though the overall number of fatalities decreased by 19%. [1] Therefore, it is possible that the number of fatalities of elderly people in traffic crashes will further increase due to an aging society. As a result, protection for the elderly in traffic crashes is critical.

A previous study done by NHTSA analyzed the National Automotive Sampling System Crashworthiness Data System (NASS-CDS) and found that the percentage of drivers sustaining Maximum Abbreviated Injury Scale (MAIS) 4+ injuries relative to the number of drivers involved in crashes is significantly larger for the elderly population (greater than 65 years old) compared to occupants between 25 and 44 years old, 1.85% compared to 0.76%, respectively [3]. Specifically, for left-side impacts without rollover the percentage of elderly occupants becomes even larger and is the largest percentage of all crash modes. This suggests that the protection of elderly drivers involved in left-side impacts is important.

One of the factors that likely contributes to the high probability of severe and fatal injuries to elderly occupants is the increased fragility of their bones. For example, Agnew et al. [4] showed that in whole rib bending tests, the tensile failure strain in the rib significantly decreases with age. This group also showed that body height had a positive relationship with both peak force and total fracture energy. [5] Therefore, shorter occupants, such as small elderly females, may have a higher probability of severe and fatal injuries. Ramachandra et al. [6] revealed that the probability of AIS3+ injury in side impact crashes also depends on sex. According to the study, in near-side impacts, the probability of injury to the thorax and the ribs were significantly higher for females than for males within the elderly population, (over 60 years of age). All of these studies suggest that small, older female drivers in near-side impacts are more susceptible to thoracic injuries, particularly rib fractures.

Despite the growing importance to better understand how to protect elderly females in near-side impacts, few studies have investigated this impact configuration. A recent study by Shurtz et al. [7] conducted side impact sled tests using two small elderly female post-mortem human subjects (PMHS). These sled tests included realistic boundary conditions of a typical near-side impact including: seat-belt with a pretensioner, side airbag and intruding car door. In addition, there has only been one validated Human Body Model (HBM) representing an elderly female published to date [8]. This elderly female HBM was validated against a side sled test with rigid wall, which is not a realistic boundary condition. Unfortunately, at this time there is not a validated small elderly female HBM that could be used to test safety systems in near side impact scenarios. Therefore, the objective of this study was to develop a HBM of a small elderly female occupant under realistic boundary conditions in the near side.

METHOD

A two-phase approach, model creation and model validation, was taken to achieve our goal as shown in Figure 1. During the model creation phase, a three-step approach was taken including: (1) scale a whole body model from a 50th male (AM50) to a 5th female (AF5), (2) create a single rib model to match previous rib experimental testing, and (3) create an average elderly female rib model using literatures. The modeled fragile female ribs were then used in the creation of the AF5 model and validated. Validation was accomplished in terms of prediction of rib fractures and thoracic injury severity using three different experiments: (1) single rib experimental bending test, (2) a whole-body thoracic impact test series and (3) whole-body PMHS side sled test using realistic boundary conditions.

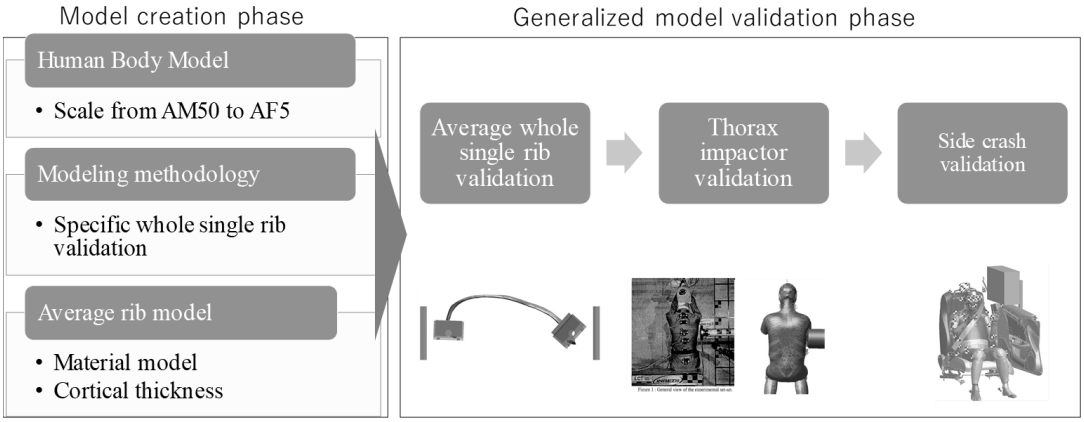

Figure 1. Scheme of development of HBM for elderly female

Model Creation Phase (Whole Human Body Model)
The Human Body Model (HBM) AM50 was evaluated as an elderly occupant by Dokko et al.[9]. This model served as the baseline model that was then adapted with finite element capable software, LS-DYNA (version R7.1 LSTC, Livermore, CA, USA) to convert it into the AF5 model. The thorax of the AM50 model had been developed based on a CT of a single elderly male with average body size, 175 cm in height and a mass of 77kg. The material properties used to represent the cortical bone located in the ribs were determined using tensile test results reported by Kemper et al. [10][11]. The AM50 elderly model was validated against thoracic impact tests documented in ISO-TR9790 (1997) [12] along with side and frontal sled tests conducted by Lessley et al. [13] and Shaw et al. [14]. The biofidelity score for these validation tests ranged from 0.23 - 1.18 based on the assessment scheme proposed by Rhule et al. [15].

The AM50 HBM was scaled to that of a small female body size (AF5). The model was scaled to 0.86 times relative to the x, y, and z axes equally to accomplish a stature of 151 cm. In addition, the densities of the internal organs were adjusted to match the target total body mass which was 47 kg based on a dataset published by Robbins et al. [16]. The skeletal model of the thorax of the AF5 was then compared with a statistical small female model published by Wang et al. [17]. It was found to be close to the statistical rib-cage geometry as shown in Figure 2. The AF5 thorax was approximately7% larger in width and 0.5% larger in depth.

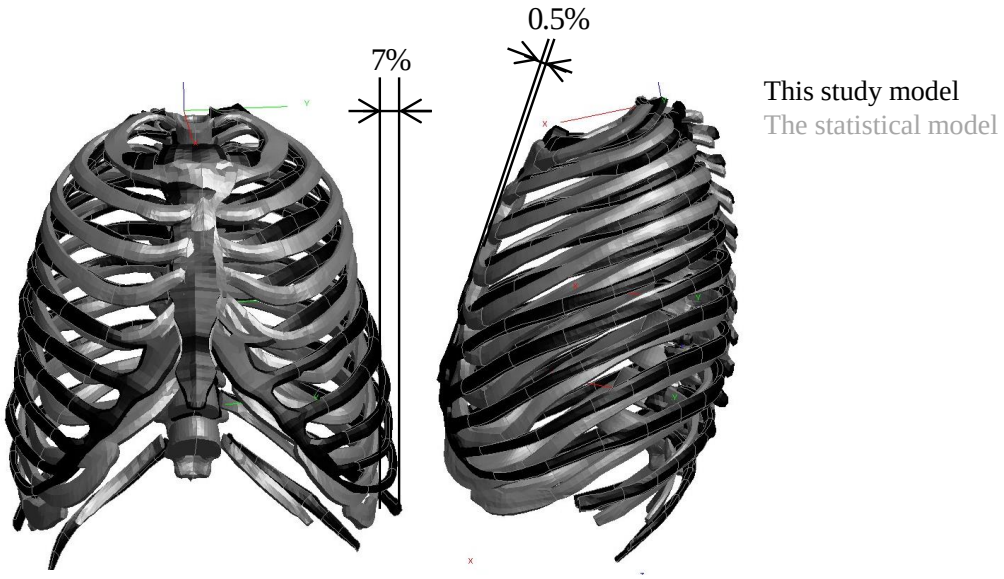

Figure 2. Comparison between thoracic skeletal morphology in the simulation and in the statistical model for the small elderly female

Model Creation Phase (Determination of modeling methodology for whole single rib – Parametric study)
As stated one of the validation parameters for the AF5 model is intended to be the number and location of rib fractures. Therefore, it was critical to model the correct material property for rib cortical bone and validate a whole single rib against published experimental testing. Whole single rib tests were simulated to determine the most appropriate rib modeling methodology; variables investigated included: number of sections along the length of the rib, cortical thickness of each section and the best material properties to use for cortical bone. Experimental bending tests using a whole 6th rib published by Agnew et al. [4] were simulated and the results were compared with the experimental results to determine the best modeling methodology.

Two ribs from two different female subjects used in the published whole bone experimental tests were selected to model and simulate. The two selected experimental ribs, subject 1 and subject 2, were scanned using both a FARO laser scanner, as well as computed tomography (CT). The images were used to create computer-aided design (CAD)

models of the surface of the ribs using Mimics (Ver. 12.0, Materialise, Leuven, Belgium). Cortical bone models were then developed with shell mesh and filled in with solid mesh to reproduce the trabecular bone from the CAD models. Cortical thicknesses of each rib was measured using both CT data and histological rib cross-section data. Each rib was sectioned into 8 cross-sections equally divided along the length of the rib. For each of the 8 cross-sections, four thicknesses were calculated: cutaneous, pleural, superior and inferior. The cortical thicknesses were measured for all 8 cross-sections from the CT images. However only one cross section of each rib, located 67% along the length of the rib, underwent histological analysis. The CT scan had an in-plane resolution of 0.146 mm, while the histological analysis had a resolution of 1,446 pix/mm (0.000692 mm/pix) as published by Agnew et al. [4]

The test set-up of the whole-rib simulation tests matched the experimental tests. The vertebral and sternal ends of the rib model were constrained in pots which were oriented perpendicular to the rib as it entered the pot. The pots on both ends were allowed to rotate about the z-axis. In addition, the sternal end could be moved posteriorly along the x-axis, representing a frontal crash. The reaction force was measured at the vertebral end of the rib in the experimental tests by Agnew et al. [4] and also in the simulation along with the displacement of the sternal end of the rib for a direct comparison to calibrate the model. As mentioned, a parametric study was conducted using this simulation changing three key parameters: number of sections along the length of the rib, cortical thickness of each section and the best material properties to use for cortical bone. The parametric study matrix is shown in Table 1.

Table 1.
Parametric study matrix of bending simulation and results

Case ID		Model 1	Model 2	Model 3	Model 4
Parameter	Number of total divisions in the rib	16	32	32	32
	Thickness source	CT	CT	Function between microscope and CT	Function between microscope and CT
	Material properties	MAT24 Tension	MAT24 Tension	MAT24 Tension	MAT124 Tension & Compression

<u>Parameter 1 – Number of divisions in the rib:</u> As stated earlier, the two modeled ribs were portioned into 8 sections longitudinally along the length of the rib. For each longitudinal section, the cortical bone was then broken into 4 sections circumferentially. The first variable the parametric study evaluated was how many divisions of cortical bone were needed to adequately model the experimental ribs. A comparison between a simplified model with 16 cortical bone divisions (Model 1) and a more detailed model of 32 cortical bone divisions (Model 2, Model 3 & Model 4) as shown in Figure 4. The simplified model only looked at using 4 of the longitudinal cross-sections versus all 8.

<u>Parameter 2 – Cortical bone thickness source:</u> Two types of cortical bone thickness values were applied. As mentioned previously, thickness values came from both the CT scans, in all 8 longitudinal cross-sections, and a histological measurement, at a single cross-section. On the cross-section that had both a CT measurement and a histological measurement, a correlation between the two measurement techniques was calculated. The relationship between the measured histological cortical thickness, which is considered the gold standard for measuring cortical bone thickness, and the CT thicknesses was calculated as shown in Table 2, Equation 1 and Figure 3. The relationship as defined in equation (1) had a R square value of 0.83 certifying good correlation between the data when using a linear approximation based on a least-squares fit. Model 1 and Model 2 used cortical bone thicknesses as measured using the CT scans only, while Model 3 and Model 4 used the function as defined in Equation 1 to calculate the thickness of each cortical bone segment.

$$D_{mod} = 1.2253 * D_{ct} - 0.6302 \qquad \text{(Equation 1)}$$

Table 2.
Cortical thickness measurement between CT and Histological measurement

	Thickness source	CT (mm)	Histological measurement (mm)
Subject 1	Superior cortex	0.77	0.21
	Cutaneous cortex	0.86	0.25
	Inferior cortex	0.74	0.14
	Pleural cortex	1.00	0.63
Subject 2	Superior cortex	0.49	0.19
	Cutaneous cortex	1.17	0.81
	Inferior cortex	0.66	0.47
	Pleural cortex	1.24	0.97

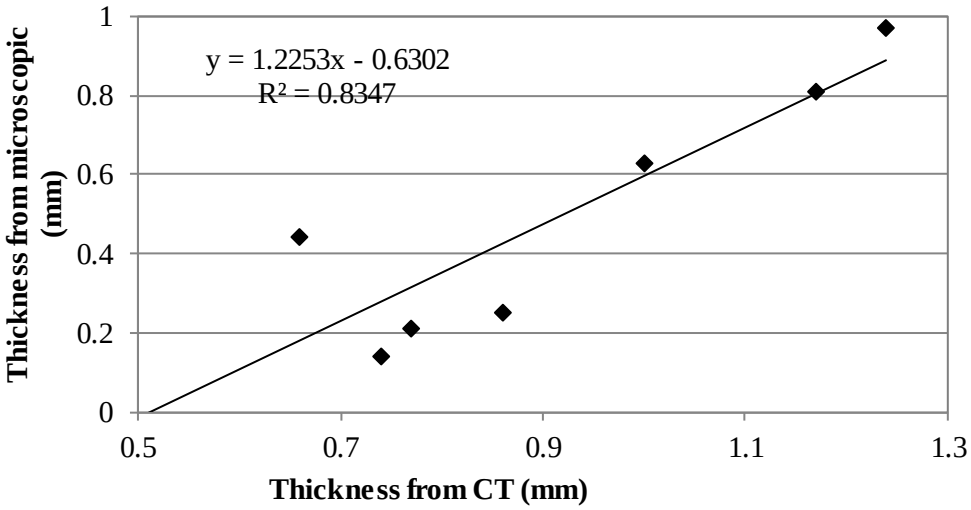

Figure 3. Relationship between measurements scanned from CT and from microscope

Parameter 3 – Cortical bone material property: The material properties of the two tested experimental ribs were calculated from experimental coupon tests conducted by Albert et al. [18]. After the ribs were tested in the whole-rib experimental set-up, the ribs were taken to Virginia Tech University where the coupon tests were completed. The material property of the trabecular bone was applied using the same value from Dokko et al. [9]. In addition, the strain rate of cortical bone and trabecular bone was applied according to a previous study by Takahashi et al. [19] The material properties for each subject was obtained from the coupon testing published by Albert et al. [18]. Compression property was determined as 1.2 times tension property from Kemper et al. [11] For Model 1, Model 2 and Model 3, these values were all the same as shown in Table 1 as MAT24 PIECEWISE_LINEAR_PLASTICITY specifying only tension. However, in Model 4, MAT124 PLASTICITY_COMPRESSION_TENSION were applied specifying tension and compression, respectively.

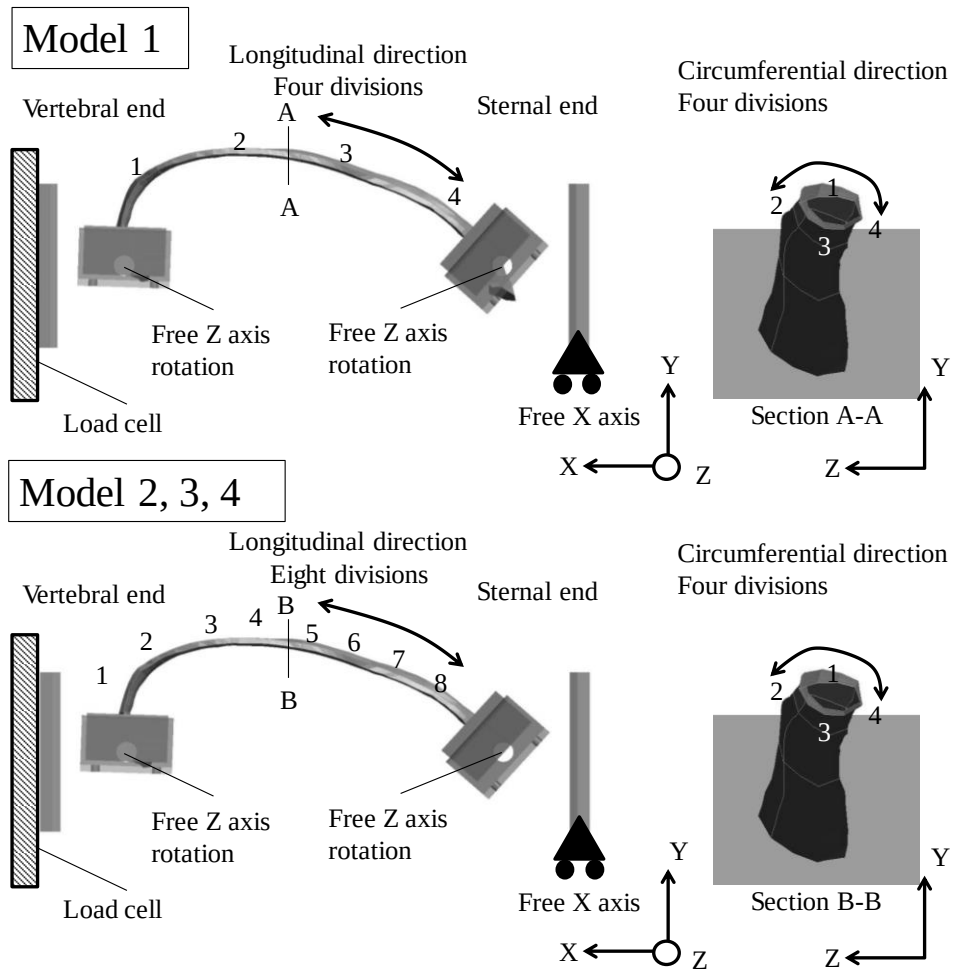

Figure 4. Bending test equivalent

Parametric Study – Method used to select the best model; As mentioned, the simulated reaction force time histories at the vertebral end of the rib were compared to the experimental data from Agnew et al [4]. The 4 versions of the model were evaluated both in terms of fracture reproducibility and force-displacement correspondence to determine the best method to model the whole-rib impact tests. The total energy, which was the total area under the force-displacement curve up to the time of fracture, was calculated and compared between each of the four parametric models and the experiment, and was used to evaluate the fracture accuracy. Also, the ratio of maximum force between simulation and experiment was used to evaluate the reaction force accuracy. Finally, the best modeling methodology was determined by averaging these two ratios. The average ratio closest to 1.0 indicated a good correlation between the simulation and the experiment.

Model Creation Phase (Determination of average material properties and cortical thicknesses for elderly female)

The representative material properties of the rib cortical bone for elderly female were determined using literatures. There are two human models for elderly female developed by Kalra et al. [20] and Iwamoto et al. [21] et al. They used the material properties for cortical thickness of rib as shown in Table 1A in Appendix. Our study used average material properties of two model. Young's modulus, Yield stress, Ultimate strain, and Ultimate stress were set by 11.1 GPa, 78.0 MPa and 0.022, respectively. The average cortical thickness was applied to median thickness value between two subjects of the bending test. Cortical thicknesses were used with average cortical thicknesses of two subjects as shown in Table.2A in Appendix. Average whole single rib were developed. Then, the average HBM were validated in next phase.

Model Validation Phase (Validation of whole rib bending test)

A whole-rib simulation test was validated using the rib bending test published by Agnew et al. [4] as detailed in the parametric methods section. The reaction force of the simulation was compared with the range of reaction forces documented in the experimental results. Simulation results were evaluated using the acronym of CORelation and Analysis (CORA) system. [22] The CORA rating is a method to evaluate the time-history signals, the reference curve (experimental result) and the predicted response (simulation result). CORA uses two methods to calculate the signals correlation: the corridor method calculates the deviation of the signal between two curves automatically created by the CORA software, while the cross-correlation method evaluates the characteristics of the signal such as phase shift, size, shape and progression. The total CORA score sums up the results of both metrics by using individual weighting factors from 0 to 1 for each metric. According to the rating stipulated in ISO/TR 18571 the resultants of the CORA score are classified into four categories: values above 0.94 are considered excellent, values between 0.94 and 0.8 are good, values between 08 and 0.58 are considered as a fair correlation and values below 0.58 are treated as a poor correlation.

Model Validation Phase (Validation of the HBM thorax in a side impact component test)

The evaluated whole-rib model was then applied to the full-body HBM for an elderly female. To validate the full-body HBM in a component level test, a lateral chest impact conducted by Talankinte et al. [23] was adopted to compare the thoracic impactor reaction force time histories. The thorax of the HBM was impacted in a lateral direction with a 150 mm diameter impactor, weighing 16 kg at a speed of approximately 6 m/s, matching the experimental conditions defined by Talankinte et al. [23] Only two female subjects (LCT02, LCT03) over 53 years old were tested in these experimental conditions. The geometric and inertial scaling method proposed by Mertz et al.[24] was performed on both subjects in order to better compare their results with the simulation. Force and time normalizing factors were calculated by Equations (2) and (5).

$$\mathrm{Rf} = (\mathrm{Rm}\ \mathrm{Rk})^{1/2} \qquad \text{(Equation 2)}$$

$$\mathrm{Rt} = (\mathrm{Rm})^{1/2}(\mathrm{Rk})^{1/2} \qquad \text{(Equation 3)}$$

where

$$\mathrm{Rm} = \mathrm{Ms}\ \mathrm{Mi}^{-1} \qquad \text{(Equation 4)}$$

$$\mathrm{Rk} = 308/L \qquad \text{(Equation 5)}$$

The mass ratio (Rm) was calculated using the total mass of the HBM (Ms), which was 47kg and the total mass of each experimental subject (Mi) as shown in equation 4. The stiffness ratio (Rk) uses a characteristic length ratio, in this scenario it is defined using chest width. Equation 8 defines RK to be the chest width of the 5th percentile elderly female HBM (308 mm) divided by chest width of each subject (L). Simulation results were then evaluated versus the experimental thoracic impacts using CORA as described in the validation of the whole-rib model.

Model Validation Phase (Validation of the HBM in a side impact sled test with realistic boundary conditions)
The published side impact sled tests with post mortem human subjects (PMHS) at an impact velocity of 28 km/h using a side airbag and simulating door intrusion (Shurtz et al.) [7] were simulated using the defined 5th percentile HBM. Comparisons between the simulation and the PMHS experiments were then conducted considering all of the following: spinal and pelvis kinematics, number of rib fractures and thoracic deflection from chest bands. The initial position of the HBM was set to match the experimental position data of each body segment and/or landmark including: head, sternal notch, olecranon and greater trochanter as shown in Figure. 5. The two PMHS responses were normalized to compare to the simulation responses using a length scale factor λz (seated height of the subjects) and a mass scale factor λm (total body mass). This normalization technique assumes equal density throughout each PMHS, so that the lateral displacement scale factor is defined by equation (6) proposed by Mertz et al.[25]

$$\lambda_y = Rm^{1/2}/\lambda z^{1/2} \qquad \text{(Equation 6)}$$

As with the whole-rib test and the thorax component test, the PMHS sled test simulation was evaluated using CORA. In addition, both the timing and location of the rib fractures predicted in the simulation were compared with those from the experimental results, when the fracture times were available in the PMHS tests.

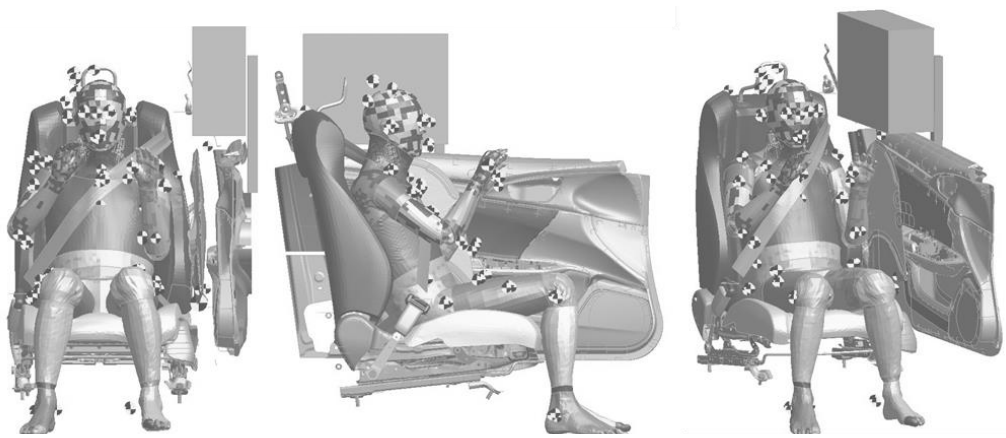

Figure 5. Comparison of seating position in the simulation with the experimental FARO data. Target mark indicates the experimental FARO data

RESULTS

Results of Parametric Study – Model Calibration
The parametric study parameters and evaluation results such as total energy ratio and max force ratio are shown in Table 4. The reaction force at the vertebral end of the rib is compared with the experimental data and shown in Figure 6. Based on the results, Model 4 appeared to be best represent the rib bending test given it has the values closest to 1.0 for both the total energy ratio and the max force ratio in this parametric study. Therefore, the modeling methodology for Model 4 was determined to be used for the validation phase of the models moving forward.

Table 4.
Parametric study matrix of bending simulation and results

		Case ID	Model 1	Model 2	Model 3	Model 4
Parameter		Number of divisions in the rib	16	32	32	32
		Thickness source	CT	CT	Function between Microscope and CT	Function between Microscope and CT
		Material properties	MAT24 Tension	MAT24 Tension	MAT24 Tension	MAT124 Tension & Compression
Evaluation	Subject1	Max force ratio	1.18	1.02	0.66	0.77
		Energy ratio	1.86	1.54	1.05	1.09
		Average ratio	1.52	1.28	0.86	0.93
	Subject2	Max force ratio	1.01	0.94	0.75	0.89
		Energy ratio	2.06	1.89	0.97	1.09
		Average ratio	1.54	1.42	0.86	0.99

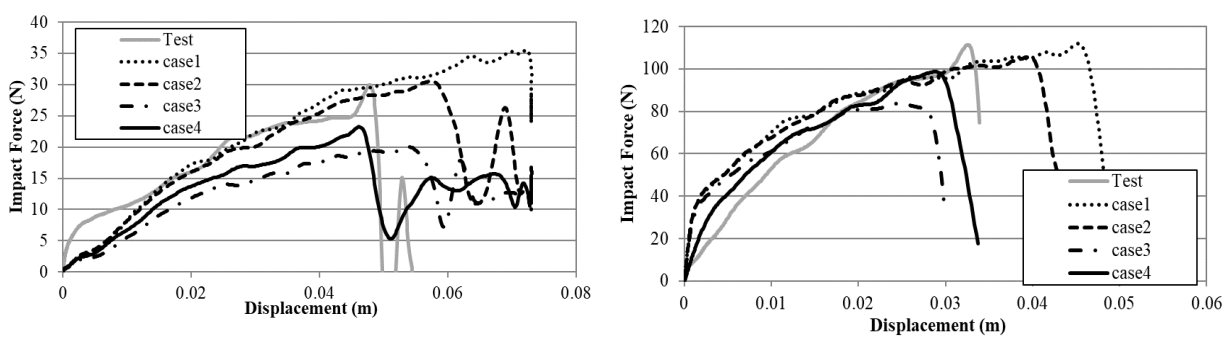

(A) (B)

Figure 6. Comparison of impactor force time history in parametric study ((A) subject1 results, (B) subject2 results)

Validation of Whole-Rib Model in Single Rib Bending Test

Figure 7 shows the comparison of the resulting force at the vertebral end of the whole rib and the total rib displacement between both experimental subject tests and the simulation with average material properties model. Peak force, which was 63 N was within the experiment results range of subject1 and subject2.

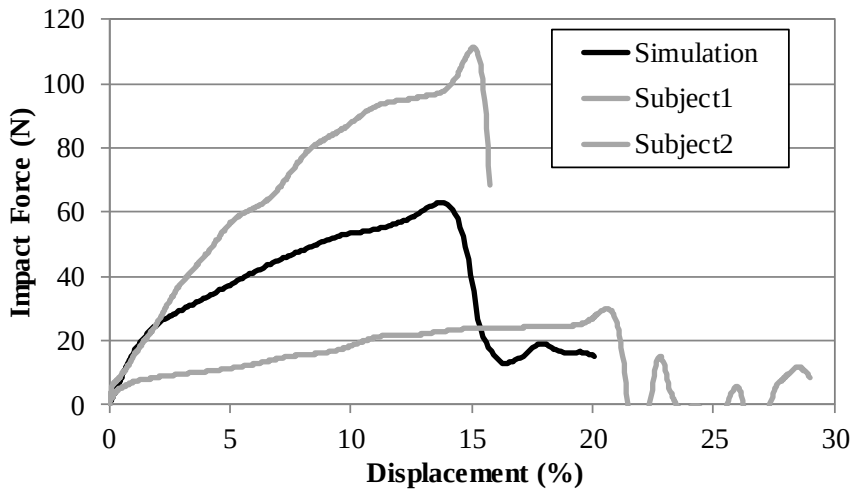

Figure 7. Comparison of bending impactor force displacement history in average rib model

Validation of Chest Side Impact Test

The modeling methodology for Model 4 was then applied to the thorax model of the HBM. Figure 8 shows the comparison of the chest impact force time history between the normalized experimental tests and simulation results. A standard deviation was calculated from the results of the normalized experiment results using two subjects. A CORA score of 0.885 is ranked "Good".

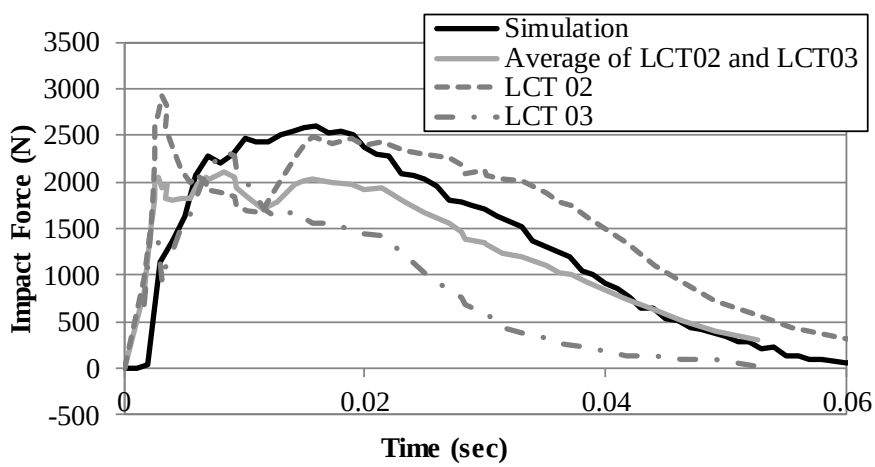

Figure 8. Comparison of impact force time history in simulation with the chest impact experiment

Validation of Side Impact Sled with Airbag

The seating position of the representative HBM showed good agreement with the experiential position point dataset as shown in Figure 5. Table 4 shows a summary of the CORA score regarding lateral displacement time histories of T1, T4, T12 and pelvis in the global coordinate system. The CORA score for lateral displacement indicates Excellent or Good, due to the range of CORA scores between 0.87-0.98. The lateral displacement time histories in the global coordinate system for each body region are also presented in Figures 9.

Table 4.
CORA Score and evaluation of lateral displacement at measurement points in sled test

Lateral displacement of body region	Corridor method	Correlation method	Total score
T1	0.99	0.89	0.95
T4	1.00	0.95	0.97
T12	1.00	0.97	0.98
Pelvis	0.86	0.87	0.87

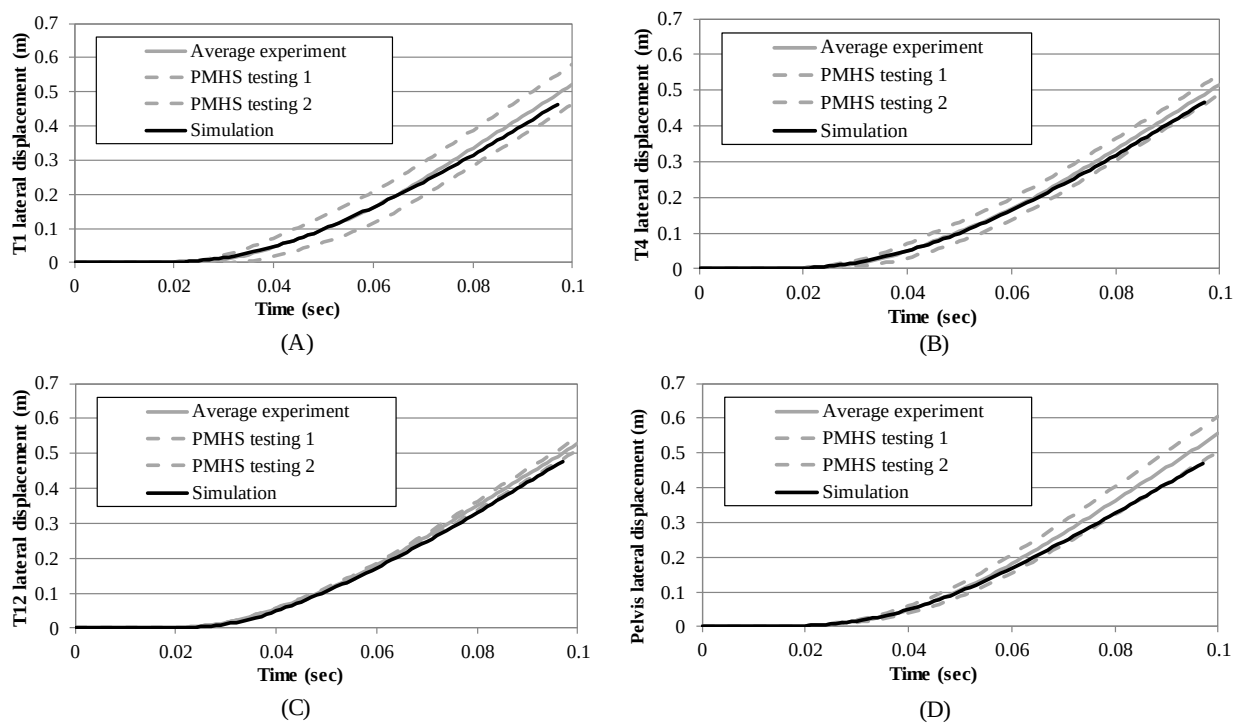

Figure 9. Comparison of lateral displacement of T1, T4, T12, and Pelvis between simulation and experiment ((A) T1 displacement, (B) T4 displacement, (C) T12 displacement, (D) Pelvis displacement)

Table. 5 shows the comparison between the fracture locations in the experiment with the simulation. In the simulation, shells of rib cortical bone were considered fractured when they reached 0.022 strain as defined by literatures. Fractures on the struck side occurred across the whole thorax, while fractures on the non-struck side occurred only in the upper and mid- thorax for both cases. The timing of rib fractures is also presented in Table 5. The first fracture occurred to the 7th anterior rib on the struck side of PMHS2 at 20 msec in both the experiment and

the simulation. Fractures on the non-struck side occurred later than fractures on the struck side. Thoracic deflection at the level of the axilla measured by the chestband were compared with the simulation results in both lateral and anterior-posterior (A/P) direction as shown in Figure 10. Maximum lateral thoracic deflection in the simulation and experiment were 14% and 15%, and both occurred at approximately 36 msec. Maximum anterior-posterior deflections were 5% and 6%, with both occurring approximately 19 msec.

Table 5.
Fractured rib location and timing in the sled test

Rib #	**PMHS1**		**PMHS2**		**Simulation**	
Fracture side	Struck	Non struck	Struck	Non struck	Struck	Non struck
Rib1						
Rib2	Fx:Ant(N/A)				Fx:Ant(28)	
Rib3	Fx:Ant(N/A)		Fx:Ant(26)	Fx:Ant(26)	Fx:Ant(23)	Fx:Ant(44)
Rib4	Fx:Ant(N/A)	Fx:Ant(47)	Fx:Ant,Post(27)	Fx:Ant(31)	Fx:Ant(28)	
Rib5			Fx:Ant.Post(21)	Fx:Ant(38)	Fx:Ant(44)	Fx:Ant(46)
Rib6	Fx:Ant(39)		Fx:Ant,Post(20)	Fx:Ant(39)	Fx:Ant(22)	
Rib7			Fx:Ant,Post(19)	Fx:Ant(N/A)	Fx:Ant(20)	
Rib8			Fx:Post(29)		Fx:Ant(28)	
Rib9					Fx:Ant(22)	
Rib10					Fx:Ant(20)	
Total number of fractured ribs	4	1	6	5	9	2

Fx=fracture, Ant=anterior, Post=posterior, ( ) = time of fracture msec, N/A= unknown

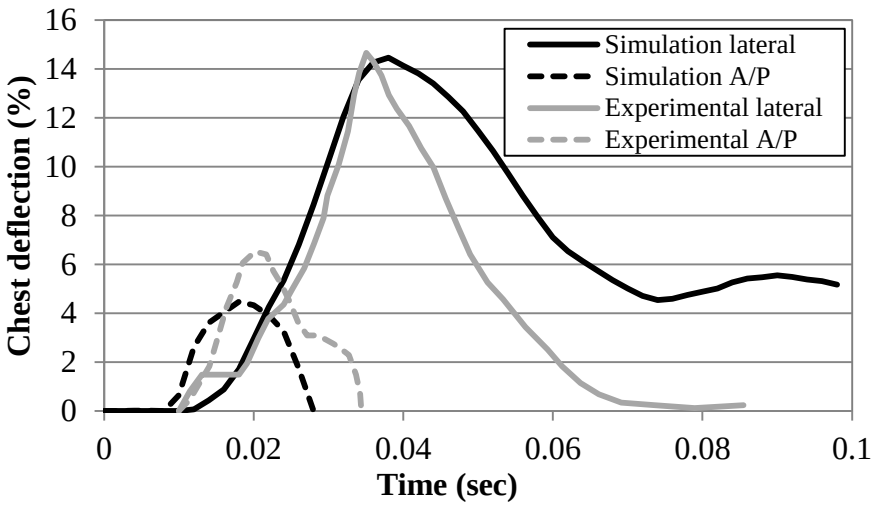

Figure 10. Comparison of thoracic deflection at the level of the axilla in side impact sled tests

DISCUSSION

In the parametric study, model 4 was more accurate than the other models for both subjects. It was found that number of rib divisions, thickness and material properties were significant parameters to predict rib fracture. Maximum force ratios were not effected in the parametric study. On the other hand, energy ratios were significantly effected in this parametric study. Therefore, these parameters were crucial to predict rib fractures, which means strain distribution of the rib were changed. As shown in Figure 11, increasing the number of rib divisions (Model 2) leads to more accurate energy ratios compared to in Model1. Similarly, Li et al. [26] found that use of variable cortical thickness distribution slightly decreased the failure displacement compared to the mode with constant cortical thickness. A more realistic cortical thickness distribution was crucial to predict the rib strain distribution.

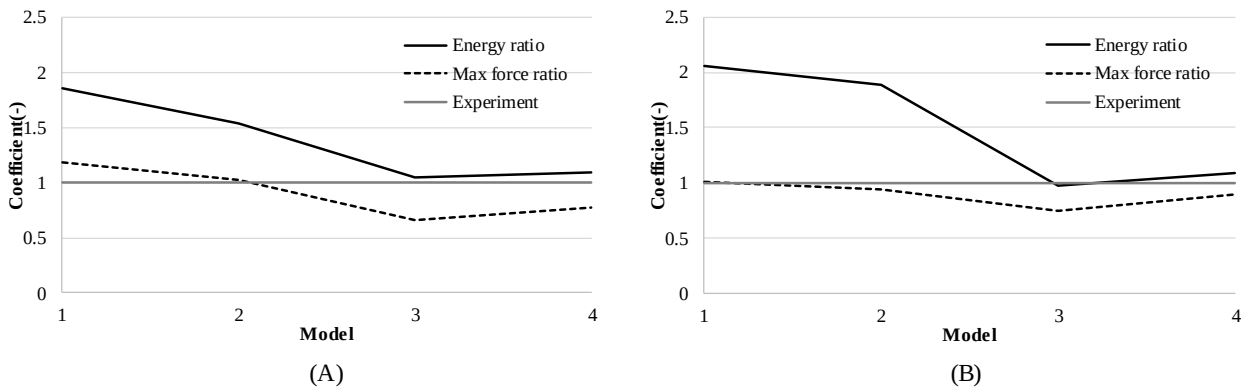

Figure 11. Comparison of max force ratio and energy ratio in parametric study ((A) subject1 results, (B) subject2 results)

Cortical thickness from the function between CT and histological measurement (Model 3) was more precise than both Model 1 and 2 in terms of energy ratio as shown in Figure 12. Actually, cortical thickness from histological measurement had a range of 0.14mm - 0.97mm. Because thresholding was used to reconstruct CT scans, cortical thickness from CT may overestimate the rib cortical thickness as can be seen in Table 2. Then rib strain may decrease so that the energy ratio was greater than the experiment. In a previous study, Perz et al. [27] found that utilizing CT images to result in greater than 100% error in cortical thickness. That difference of thickness affected mechanical response under antero-posterior loading to a single whole rib. In addition, Li et al also suggested that using for cortical thickness from a high-resolution CT data such as a micro CT would improve predicted fracture location. [26] Therefore, the resolution of the image based on cortical thickness is significant parameter for predicting rib fractures.

Considering compression (Model 4) helps to be more accuracy in this study. Kemper et al. found that cortical bone in the tibia has tension/compression asymmetry when looking at the stress-strain properties [11]. Fertschej et al. got more accuracy considering not only tension, but also additional properties (compression and shear, etc.) in the 3 point bending test using thermoplastics. [28] Shell strains-time history on the superior and inferior aspects of a middle of the rib in model 4 of parametric study were compared with those in model 3 as shown in Figure 12. Shell strain on the superior aspect of the rib in Model 4 was increasing earlier than in Model 3. Considering material asymmetry (Model 4), tensile strain distribution on the superior shell is higher than the symmetry material (Model 3) due to less the compression strain. Therefore, it is assumed strain distribution of the rib was changed when considering the compression property. It leads to be more accuracy.

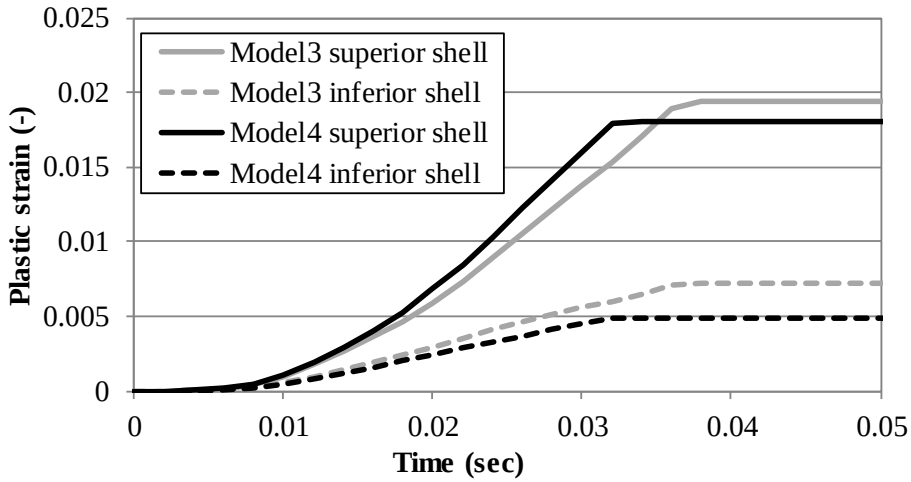

Figure 12. Comparison of plastic strain of the rib during the bending test (superior portion; inferior portion)

Regarding the whole-rib simulation validation results, the results were compared with the literature published by Agnew et al. [4] The experimental study showed peak force and peak displacement % were predicted using the following equations:

Peak force for female: FPeak = 133.58 - 0.950*Age (Equation 7)

Peak displacement for female: δPeak = 42.26 - 0.2724*Age (Equation 8)

If we assume an age of 75 years old was used for the simulation, the resulting Fpeak and δPeak would be 62.3 N and 21.3% respectively. The Average simulation results shows 68.5 N and 14% respectively, which reveal this rib model could be representative of a 75 years old of female.

This HBM showed fairly good agreement with the experiment results. A CORA score of kinematic response in the HBM is approximately 1.0, ranking Excellent. In addition, the location and timing of the fractured ribs in the simulation were compared with the experimental results. Fractures in both struck and non-struck side occurred in both simulation and in the experiments. Therefore, the simulation predicted not only the number of fractures, but also the fracture location using the deterministic method. However, humans have individual differences such as body type and varying material properties, so it should be further investigated to predict rib fractures using the probabilistic method.

CONCLUSION

The improved model for rib cortical bone was developed using thirty-two divisions of each rib, a cortical bone thickness value estimated from histological data, and material properties considering tension and compression.

The HBM developed by applying rib material properties along with geometrical scaling for an elderly female well represented the upper body kinematics, rib fractures and thoracic deflection in a side impact sled test from a published PMHS experiment.

ACKNOWLEDGEMENTS

Authors would like to grateful acknowledgement Dr. Jingwen Hu from University of Michigan Transportation Research Institute Department of Mechanical Engineering, University of Michigan (UMTRI), and Dr. Andrew Kemper from Virginia Tech-Wake Forest University for supporting their data through this study.

REFERENCES

[1] NHTSA-National Highway Traffic Safety Administration., 2017. "Traffic Safety Facts 2015." DOT HS 812 372: 1-5

[2] Ortman, M., Jennife, R., Velkoff, V., Hongan, H., 2014. "An Aging Nation: The Older Population in the United States. Current Population Reports.": 25-1140

[3] NHTSA-National Highway Traffic Safety Administration., 2005. "Characteristics of Crash Injuries Among Young, Middle-Aged, and Older Drivers." DOT HS 810 857: 44-45

[4] Agnew, A., Murach, M., Dominguez, V., Sreedhar, A., Misicka, E., Harden, A., Bolte, J., Kang, Y., Stammen, J., Moorhouse, K., 2018." Sources of Variability in Structural Bending Response of Pediatric and Adult Human Ribs in Dynamic Frontal Impacts." Stapp Car Crash Journal, Vol.62, November: 119-192.

[5] Agnew, A., Murach, M., Misscka, E., Moorhouse, K., Bolte, J., Kang, Y., 2017. "The Effect of Body Size on Adult Human Rib Structural Properties." In Proceedings of the IRCOBI Conference (Antwerp, Belgium, Sep. 11-13)

[6] Ramachandra, R., Kashikar, T., Bolte, J., 2017. "Injury Pattern of Elderly Occupants Involved in Side Crashes." In Proceedings of the IRCOBI Conference (Antwerp, Belgium, Sep. 11-13)

[7] Shurtz, B., Agnew, A., Kang, Y., Bolte, J., 2018. "Application of Scaled Deflection Injury Criteria to Two Small, Fragile Female in Side Impact Motor Vehicle Crashes." SAE International Technical Paper, April: 2018-01-0542

[8] Jin, X., Kalra, A., Hammad, A., Khandelwal, P., Porwal, V., Shen, M., Yang, K., 2018. "Development and Validation of Whole-Body Finite Element Occupant and Pedestrian Models of a 70-Year-Old Female" In Proceedings of the IRCOBI Conference (Athens, Greece, Sep. 12-14)

[9] Dokko, Y., Yanaoka, T., Ohashi, K., 2013. "Validation of Age-Specific Human FE Models for Lateral Impact." SAE International Technical Paper: 2013-01-1242.

[10] Kemper, A., McNally, C., Kennedy, E., Manoogian, S., Rath, A., Ng, T., Stitzel, J., Smith, E., Duma, S., Matsuoka, F., 2005. "Material Properties of Human Rib Cortical Bone from Dynamic Tension Coupon Testing." Stapp Car Crash Journal, Vol.49, November: 199-230.

[11] Kemper, A., McNally, C., Kennedy, E., Manoogian, S., Duma, S., 2007. "The Material Properties Of Human Tibia Cortical Bone In Tension And Compression: Implacations For The Tibia Index." In proceeding of International Technical Conference on the Enhanced Safety of Vehicles Conference (ESV) (Lyon, France, June. 18-21)

[12] ISO/TC22/SC12/WG5., 1997. "Road Vehicles - Anthropomorphic Side Impact Dummy – Lateral Impact Response Requirements to Assess the Biofidelity of the Dummy." Document N455-Revision 4

[13] Lessley, D., Shaw, G., Parent, D., Arregui-Dalmases, C., Kindig, M., Riley, P., et al. 2010. "Whole-Body Response to Pure Lateral Impact." Stapp Car Crash Journal, Vol.54: 289-336

[14] Shaw, G., Parent, D., Purtsezov, S., Kerrigan, J., Shin, J., Crandall, J., Zama, Y., Ejima, S., Kamiji, K., Yasuki, T., 2009. "Frontal Impact PMHS Sled Tests for FE Torso Model Development." In Proceedings of IRCOBI Conference (York, United Kingdom, Sep. 9-11)

[15] Rhule, H., Maltese, M., Donnelly, B., Eppinger, R., Brunner, J., Bolte, J., 2002. "Development of a New Biofidelity Ranking System for Anthropomorphic Test Devices." Stapp Car Crash Journal. Vol 46: 477-512

[16] Robbin, D., 1983. "Anthropometric Specifications For Small Female And Large Male Dummy, Volume3." FINAL REPORT Oct: UMTRI-83-53-3

[17] Wang, Y., Cao, L., Bai, Z., Reed, M. Rupp, J., Hoff, C., Hu, J., 2016. "A Parametric Ribcage Geometry Model Accounting for Variations Among the Adult Population." Journal of Biomechanics. Vol 49: 2791-2798

[18] Albert, D., Kang, Y., Agnew, A., Kemper, A., 2017. "A Comparison of Rib Structural and Material Properties from Matched Whole Rib Bending and Tension Coupon Tests." In Proceedings of the 2017 IRCOBI Conference (Antwerp, Belgium, Sep. 11-13)

[19] Takahashi, Y., Kikuchi, Y., Konosu, A., Ishikawa, H., 2000. "Development and Validation of the Finite Element Model for the Human Lower Limb of Pedestrians." Stapp Car Crash Journal. Vol 44: 2000-01-SC22

[20] Kalra, A., 2017 "Development of an Elderly Female Torso Finite Element Model for Restraint System Research and Development Applications." Doctoral thesis. Wayne State University.

[21] Iwamoto, M., Nakahira, Y., Kimpara, H., Min, K., 2013. "Development of a Finite Element Model of 5th Percentile Female with Multiple Muscles and Its Application to Investigation on Impact Responses of Elderly Females." In Proceeding of the 23rd International Technical Conference on the Enhanced Safety of Vehicles (ESV) (Seoul, Republic of Korea, May 27-30)

[22] Gehre, C., Gades, H., Wernicke, P., 2009. "Objective Rating of Signals Using Test and Simulation Responses." In Proceedings of the 21st International Technical Conference on the Enhanced Safety of Vehicles Conference (ESV) (Stuttgart, Germany, June. 15-18)

[23] Talantikite, Y., Bouquet, R., Ramet, M., Guillemot, H., Robin, S., Voiglio, E., 1998. "Human Thorax Behaviour for Side Impact: Influence of Impact Masses and Velocities." In Proceedings of International Technical Conference on the Enhanced Safety of Vehicles Conference (ESV) (Ontario, Canada, May31-June 4)

[24] Mertz, H., 1984. "A Procedure for Normalizing Impact Response Data." In Proceedings of SAE International Congress and Exposition.: 840884

[25] Mertz, H., Irwin, A., Melvin, J., Stalnaker, R., Beebe, M., 1989. "Size, Weight and Biomechanical Impact Response Requirements for Adult Size Small Female and Large Male Dummies in Automotive Frontal Impacts." SAE, Warrendale, PA, : 133-144

[26] Li, Z., Kindig, M., Subit, D., Kent, R., 2010. "Influence of Mesh Density, Cortical Thickness and Material Properties on Human Rib Fracture Prediction." Medical Engineering & Physics, Vol 32, November: 998–1008

[27] Perz, R., Toczyski, J., Subit, D., 2015. "Variation in the Human Ribs Geometrical Properties and Mechanical Response Based on X-ray Computed Tomography Images Resolution." Journal of the Mechanical Behavior of Biomedical Materials. Volume 41, January: 292-301

[28] Reithofer, P., Fertschej, A., Hirschmann, B., Jilka, B., Rollant M., 2018. "Material Models for Thermoplastics in LS-DYNA from Deformation to Failure." In Proceedings of International LS-DYNA User Conference (Michigan, United states, June 11-12)

APPENDIX

Table 1A.
Average rib cortical material properties for elderly female

Data source	Young Modulus [GPa]	Yield Stress [MPa]	Ultimate Strain [-]
This study (Average)	11.1	78.0	0.022
Kalra et al.	7.3	54.0	-
Kimpara et al.	14.8	101.9	0.022

Table 2A.
Cortical thickness measurement calculated to histological measurement from CT

	Thickness source	5%	13%	25%	38%	50%	67%	75%	88%
Subject 1	Superior cortex (mm)	2.18	1.44	1.80	0.56	0.44	0.24	0.49	0.41
	Outer cortex (mm)	1.94	1.49	0.90	0.49	0.29	0.36	0.46	0.44
	Inferior cortex (mm)	2.55	1.47	1.23	1.78	0.75	0.20	0.49	0.51
	Inner cortex (mm)	0.87	0.94	1.44	1.10	0.99	0.60	0.41	0.39
Subject 2	Superior cortex (mm)	0.41	1.59	0.92	1.35	1.15	0.14	0.54	0.39
	Outer cortex (mm)	1.28	0.28	1.46	1.35	0.61	0.14	0.38	0.49
	Inferior cortex (mm)	1.86	1.39	1.63	1.77	1.30	0.92	1.20	0.39
	Inner cortex (mm)	1.28	0.28	1.46	1.35	0.61	0.14	0.38	0.49
Average	Superior cortex (mm)	1.29	1.52	1.36	0.95	0.80	0.19	0.52	0.40
	Outer cortex (mm)	1.90	1.44	1.26	1.13	0.80	0.64	0.83	0.42
	Inferior cortex (mm)	1.91	0.88	1.34	1.57	0.68	0.17	0.43	0.50
	Inner cortex (mm)	1.26	1.26	1.87	1.74	1.32	0.87	0.88	0.44